JTTEE5 6:475-485

Microstructure and Mechanical Properties of Thermally Sprayed Silica/Nylon Nanocomposites

L.S. Schadler, K.O. Laul, R.W. Smith, and E. Petrovicova

(Submitted 27 December 1996; in revised form 7 April 1997)

High-velocity oxyfuel thermal spray processing was used to produce ceramic/polymer (silica/nylon) nanocomposite coatings. By optimizing spray parameters such as nozzle design, spray distance, oxygen-to-fuel ratio, powder feed position, and substrate cooling, dense coatings with relatively uniform particulate distribution could be achieved. Compared to pure nylon coatings, scratch resistance improved by 30% and wear resistance by 50%. The surface chemistry of the silica filler affected the final coating properties. Silica particles with a hydrophobic (methylated) surface resulted in better mechanical properties than those with a hydrophilic (hydroxylated) surface.

Keywords filler, HVOF, nanocomposites, nylon 11, polymer coatings, thermal spraying

1. Introduction

Polymer coatings are used in a growing range of applications, including passivation, wear resistance, chemical resistance, and even for nonstick cookware. Despite their use, the properties of these coatings are often limited by poor scratch resistance (which is related to their low modulus and low tensile strength) and high water and gas permeability.

It has been shown that both scratch resistance and permeability can be improved by the addition of nanoparticulate ceramics to the polymer (Ref 1-4). In addition, at a given level of particulate loading, the mechanical properties improve as the particle size decreases. For example, in a study by Sumita et al. (Ref 5), the yield stress of nylon filled with silica decreased by 10% compared to pure nylon when the particulate size was 220 μm and increased 20% when the particulate size was 7 nm.

To process nanoparticulate ceramic/polymer composites, a low viscosity is needed to disperse the nanoparticles and to spread the coating. This requires either that the polymer be raised to high temperatures or that large amounts of solvent be used. The difficulty with dispersing the particulate by melt mixing with the polymer is that the viscosity of the melt increases dramatically with the addition of the nanoparticulate. Therefore, the temperature of the melt must be very high to lower the viscosity sufficiently for mixing, thus degrading the polymer. In addition, thermal treatments to coat substrates with the polymer/ceramic mixtures require placing the parts being coated in an oven. This precludes applying coating in the field or on very large surfaces. On the other hand, the use of solvents for dispersion and coating is a problem because many solvents are volatile and pollute the environment.

A relatively unexplored solution to the processing problems of ceramic/polymer nanocomposites is thermal spraying. During a thermal spray process, the polymer particles are melted in a thermal jet, heated either by a plasma or via combustion, and then are accelerated against a substrate. The polymer viscosity is reduced in flight, and the powders "splat" against a substrate. No solvent or postprocessing is required to spread the coating.

Others have shown that plasma spraying (Ref 6) can be used to process pure nylon coatings; however, no investigator has reported processing of the nanocomposite polymers. The goal of this study is to overcome the processing limitations of low-volume-fraction nanocomposites by using thermal spray processing, in particular high-velocity oxyfuel (HVOF) spraying, to make nanoparticulate-ceramic-reinforced polymer coatings consisting of fumed silica reinforcing nylon 11. The HVOF system was selected over other thermal spray processes because the high velocity of the powders in flight causes large particle deformation to occur on impact against the substrate even if the polymer is still relatively viscous. Therefore, it was believed that the polymer could be processed below its degradation temperature, where the high velocity may assist with the distribution of the ceramic particles.

In this paper, ceramic/polymer (silica/nylon 11) nanocomposite coatings were processed using HVOF thermal spraying, and the scratch and wear resistance of the coatings was evaluated. Nozzle design, spray distance, oxygen-to-fuel ratio, powder feed position, and substrate cooling were all varied to optimize and understand the effects of varying thermal input into the polymer powder. Special attention was paid to the thermal treatment of the powders in flight and after deposition. In addition, nanosized silica particles with hydrophobic and hydrophilic surfaces were used to analyze the effect of surface chemistry on mechanical properties.

L.S. Schadler, Department of Materials Science and Engineering, Rensselaer Polytechnic Institute, Troy, NY 12180-3590, USA, Fax (518) 276-8554; **K.O. Laul, R.W. Smith,** and **E. Petrovicova,** Materials Engineering Department, Drexel University, Philadelphia, PA 19104, USA, Fax (215) 895-6760.

2. Experimental Approach

2.1 *Materials*

Nylon 11 (French Natural ES; Elf Atochem North America, Inc., Philadelphia, PA) was chosen as the matrix material because of its relatively high corrosion resistance and relative thermal stability. The ceramic particle reinforcement was 7 nm R812 and 12 nm A200 silica powders treated to be either hydrophobic or hydrophilic, respectively.

In order to partially aid in distribution of the ceramic filler and to be able to powder feed the nylon and silica simultaneously, the nylon and silica particles were dry ball milled together for 48 h in a ball mill using ER 120A zirconia balls with a sphericity of 0.7 and Vickers microhardness of 7 to 9 GPa. Scanning electron microscopy/energy-dispersive x-ray (SEM-EDX) silica mapping confirmed that this procedure mechanically embedded the smaller silica particles near the surface of the nylon powder particles, but did not completely distribute the silica within the nylon particles. A schematic of the subsequent nylon/silica composite particles is shown in Fig. 1. Mechanical milling was also found to improve the safe handling of the silica particles during processing since the embedded silica could not easily become airborne.

Table 1 Powders used for spraying

Powder No.	Composition, vol %	
	Nylon 11	Silica (type)
1	100	0
2	90	10 (hydrophobic)
3	90	10 (hydrophilic)
4	85	15 (hydrophobic)
5	85	15 (hydorphilic)

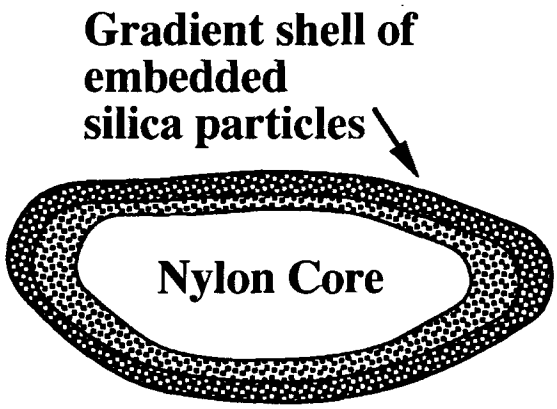

Fig. 1 Schematic showing the distribution of silica particles in nylon after ball milling

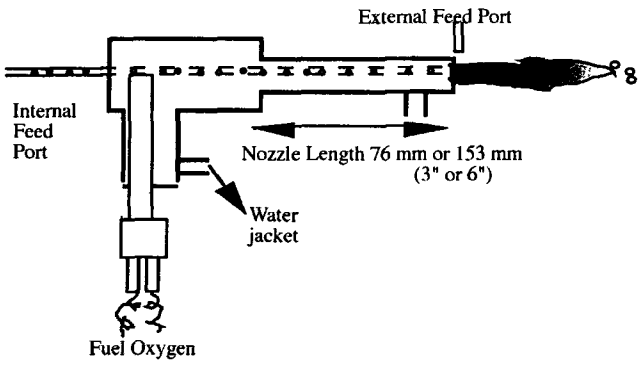

Fig. 2 Schematic of the HVOF gun, illustrating internal and external powder feed, nozzle, gas inlets, and spray distance

The nylon 11/silica nanocomposite layers were deposited as coatings onto aluminum substrates to conduct the wear and scratch tests. Prior to spraying, the aluminum substrates were cleaned in an ultrasonic bath. Five variants of composite powders, listed in Table 1, were used to produce the coatings. The composition of each powder mixture was determined from the weights of the individual components before milling. Careful examination after ball milling, which was conducted in a closed ceramic container, revealed no appreciable amount of free silica remaining. Scratch tests were conducted on three 25.4 by 75.2 by 3 mm (1 × 3 × 0.125 in.) flat aluminum coupons; wear tests were performed on two aluminum circular disks that were 75.2 mm (3 in.) in diameter and 3 mm (0.125 in.) thick.

2.2 *Thermal Spray*

In order to understand the optimum spray conditions, the HVOF nozzle design, powder injection point, fuel/oxygen ratio, spray distance, and substrate cooling were all varied, and attention was paid to the effect of each on (1) thermal input into the powders in flight (evaluated by swipe test and coating structural evaluations) and (2) thermal input into the substrate (evaluated by thermal conductivity measurements and coating appearance). Thermal input in flight melted the particles, leading to high degrees of particle deformation (flattening and splatting) upon impact, whereas thermal input into the substrate fused the particles together after deposition. In either case, however, the polymer was found to degrade if the exposure temperature was too high.

2.2.1 Nozzle Design

Figure 2 shows a schematic of an HVOF gun for reference. Two nozzle lengths were tested: 153 and 76 mm (6 and 3 in.). Both nozzles had a diameter of 8 mm ($\frac{5}{16}$ in.). Other work (Ref 7) has shown that the length of the nozzle controls the dwell time of the particles in the 2000 °C+ combustion environment, and the nozzle diameter controls the final particle velocity. Therefore, a shorter nozzle would decrease the thermal input into the powders in flight, and a smaller nozzle diameter would increase particle impact velocity. These nozzle parameters thus control the in-flight particle thermal treatment while not directly affecting the thermal input into the substrate.

2.2.2 Powder Injection

The powder was fed into the HVOF gun in either an external or internal mode (Fig. 2). The rationale behind external feed was to reduce the temperature of the powder particles in flight by eliminating particle exposure to the combustion process inside the nozzle, where the temperatures are highest. It was difficult to ensure that the powder was entrained in the flame core by using

external feed. Satisfactory powder trajectories, however, were obtained. The powder injection point, which did not directly affect the thermal input into the substrate, was another independent control on in-flight thermal input.

2.2.3 Fuel/Oxygen Ratio

Hydrogen was chosen as the fuel gas because it has lower enthalpy than other hydrocarbon fuel gases and thus imparts less heat to the polymer particles. The oxygen content further defines the jet enthalpy (energy content), where the stoichiometric ratio is the ratio that achieves maximum combustion temperatures. Excess or substoichiometric oxygen contents would then lower the combustion jet temperatures.

Table 2 shows the range of fuel/oxygen ratios that were tested to determine proper ratios for depositing the pure nylon 11 polymer. It was subsequently found that these values were appropriate for obtaining good nylon/silica composite coating morphology. Note also that the ratio was not stoichiometric.

2.2.4 Spray Distance

The spray distance was a significant parameter by which thermal input into the substrate was controlled. The greater the substrate/nozzle exit distance, the cooler the substrate/coating surface remained. In addition, the longer the polymer particles remained in the expanding combustion jet, the more time the particles had to heat.

Table 2 Conditions used to optimize spray parameters for nylon 11 coatings

Run No.	Nylon, wt %	Hydrogen flow rate at 0.83 MPa, L/min	Oxygen flow rate at 0.83 MPa, L/min	Spray distance, mm
1	100	300	600	150
2	100	300	600	150
3	100	300	600	150
4	100	400	600	200
5	100	400	600	200
6	100	400	600	200
7	100	500	600	250
8	100	500	600	250
9	100	500	600	250

Constant parameters	
Powder carrier gas	Nitrogen
Powder carrier gas flow	20 L/min at 0.69 MPa
Powder flow	9 rev/min
Substrate cooling	Water-cooled chill block
Number of cycles	3 cycles at 10 passes per cycle
Step size per pass	3.2 mm
Powder preparation	Vacuum dried at 80 °C for 24 h

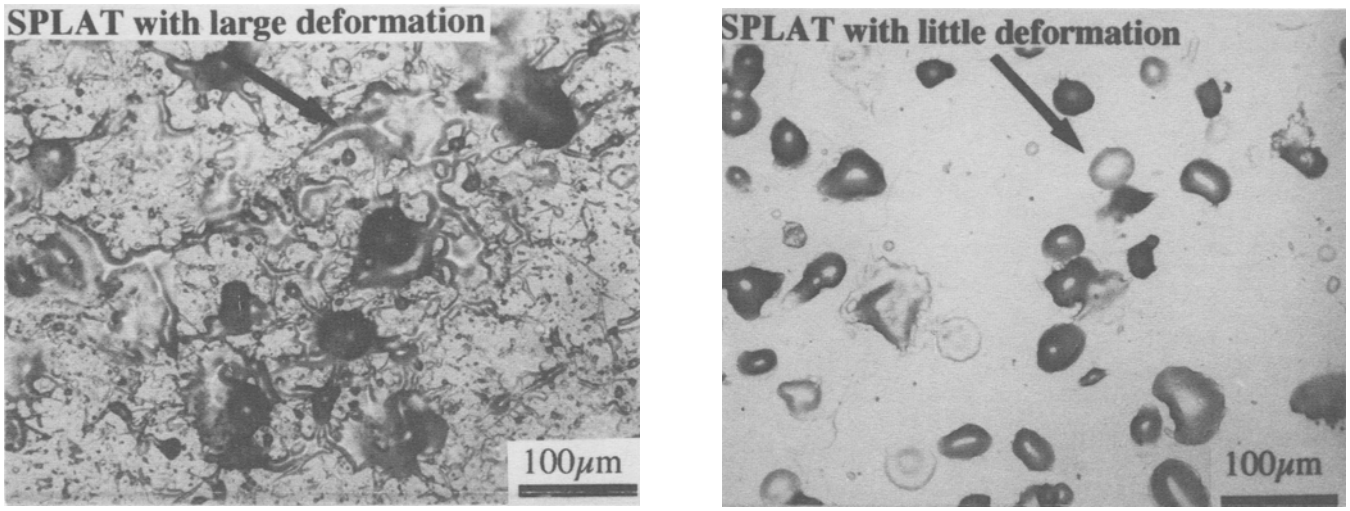

(a) (b)

Fig. 3 Results of swipe test. (a) Particles that splatted well. (b) Particles that exhibited poor splatting

2.2.5 Substrate Cooling

A further parameter to control substrate temperature was to rapidly move the coating surface or actively cool the substrate. Substrate temperature was controlled by coating the deposit onto a cylinder that was rapidly rotated in the jet and/or actively cooling the substrate by mounting it on a water-cooled copper chill block.

2.3 *Deposit Characterization*

2.3.1 Swipe Test

The swipe test, a high-speed single pass with gun over the substrate, allowed observation of the condition of individual particles upon impact (splats) without the effect of continual heating of the substrate, as may occur in a continuous coating process. In the test, glass slides were mounted in the path of the gun; after one high-speed pass, the slides were removed and the splats observed under an optical or SEM microscope. Figure 3 shows the difference between particles that were well melted in flight and deformed significantly (Fig. 3a) and those that did not melt in flight and did not deform or splat sufficiently to produce a good coating morphology (Fig. 3b). A smooth, highly deformed, disk-like particle is indicative of good melting in flight because its viscosity was low enough to permit good flow deformation upon impact. A particle that is still rounded is indicative of high viscosity with little subsequent deformation upon impact and thus shows insufficient in-flight heating.

2.3.2 Molecular Weight (Viscosity)

The molecular weight of the polymer was measured by solution viscometry before and after spraying to determine whether degradation had occurred. Solution viscometry is based fundamentally on an Einstein equation that shows that the presence of particulate in a liquid will increase the viscosity as a function of particle size and particle concentration. If polymer molecules are considered as impermeable polymer coils, then the viscosity of a polymer/solvent solution will be proportional to the length of the polymer chain (or its molecular weight).

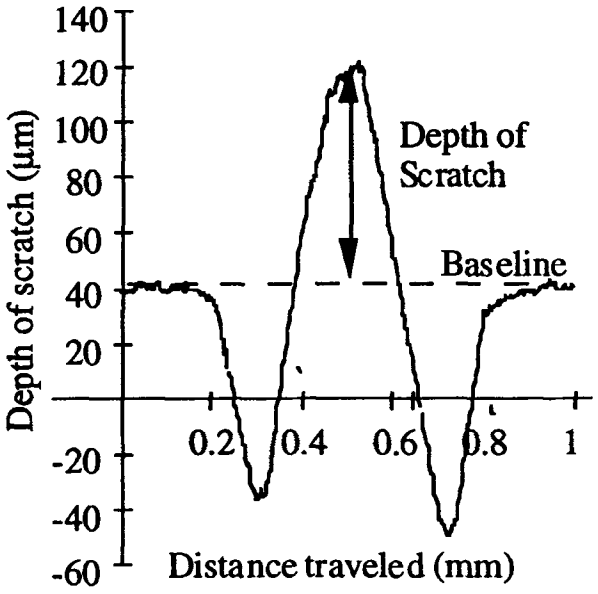

Fig. 4 Example of a scratch profile

Solution viscometry uses a capillary viscometer to measure the viscosity of several dilute solutions of polymer and solvent. By extrapolation of the viscosity at discrete concentrations of polymer down to a concentration of zero, the intrinsic viscosity, η, of the polymer can be determined. The average molecular weight, M_v, can be calculated from the Mark-Houwink parameters, a and K, and the inherent viscosity:

$$\eta = K[M_v]^a \quad \text{(Eq 1)}$$

The Mark-Houwink parameters are specific for each polymer solvent combination. An increase in molecular weight (viscosity) indicates that degradation has occurred by cross-linking; correspondingly, a decrease in molecular weight (viscosity) indicates that degradation has occurred by chain scission (Ref 8). A more complete description of solution viscometry can be found in many introductory polymer textbooks, including Ref 8.

Degradation can also be observed from a change in the color of the coating. A change from clear/white to tan or brown indicates degradation.

2.3.3 Coating Structure

The degree of deposit/coating porosity, its adhesion to the substrate, and the distribution of the particulate ceramic in the coating were evaluated qualitatively on polished cross sections of the coated aluminum flat coupons. These were mounted and then viewed in an optical microscope. The initial nylon and as-ball-milled nylon/silica powders were also observed in an SEM to determine particle structures prior to HVOF treatment.

2.3.4 Wear Tests

Sliding pin-on-disk (POD) wear tests were conducted on the deposited ceramic/polymer nanocomposite coatings using an AMTI Model C room-temperature tribometer (Advanced Mechanical Technology, Inc., Watertown, MA), which conformed to ASTM G 99-90. The apparatus consists of a rotating/oscillating spindle on which the coated disk was mounted. A stationary ball holder was used to hold the spherical (ball) counter body and apply the normal load. To avoid variations in results due to surface roughness, the coatings were polished to a surface roughness of <6 μm prior to the test. In all tests, a 10 N normal load was applied through a 10 mm diam steel ball counter body (AISI 52100) loaded onto the coated disk surface at a track radius of 21 mm. The disk surface was then rotated at 309 rev/min to achieve a relative surface speed of 0.68 m/s.

The coatings were tested at room temperature in ambient air for 15,000 cycles, requiring 2913 s of run time per test. A transducer located on the holder was used to transmit the normal and frictional forces to a data acquisition system at a sampling frequency of 1 Hz. The wear test measured coating material loss/wear by measuring the wear track area using a Hommelwerke DEKTAK II profilometer (Hommelwerke GmbH, Schwenningen, Germany). The track profile was measured at four points on each of two samples representing the same coating conditions. The wear track was also observed in an optical microscope to determine the type and mechanism of wear, if possible.

2.3.5 Scratch Test

The scratch test determines coating resistance to elastic and plastic deformation by measuring the depth of a scratch formed by a loaded needle stylus that is dragged across the surface. Before the test, the coating surface was polished to a roughness of <6 μm using No. 4000 SiC grit paper. This was necessary because the as-sprayed coating roughness (≈40 μm) approximated the scratch depth obtained at low loads, which made it difficult to isolate the scratch from the surface roughness on the profilometer graph.

The test was performed using a BYK Gardner SG-8101 balance beam scrape adhesion and mar tester (BYK Gardner, Inc., Silver Spring, MD) according to ASTM D 5178-91. The tester was used to obtain scratches on the coating surface at loads varying from 0.5 to 3 kg. Figure 4 shows a typical scratch profile. To report the coating scratch resistance, the scratch depth was averaged for three coated samples, analyzing three scratch profiles per scratch per sample. Therefore, each data point is an average of nine measured values.

3. Results and Discussion

3.1 *Thermal Spray*

Observation of the as-received nylon 11 powder by SEM showed it to be granular, but rounded (Fig. 5a). Once ball milled with the silica, however, the powder became flattened (Fig. 5b) and the majority of the silica particles were embedded in the surfaces of the nylon powder. Only small amounts of loose silica particles were observed in the mixture on the SEM-EDX silica map, indicating that the starting composition of the powder mixture was preserved. Determining the starting particle morphology just prior to spraying permitted a better evaluation of the in-flight heating effects observed by the splat test.

The swipe test showed that external feeding resulted in insufficient particle heating, which caused poor splat behavior (Fig. 6). A good splat morphology (i.e., large particle deformation on impact) is known to lead to denser coatings since the flow of the particle can fill interstices left by prior splats. Thus, in order to achieve dense coatings using external powder feeding, a high flame temperature was needed to fuse the coatings. In the tests with deposits made using external powder injection, higher flame temperatures caused higher substrate temperatures. Fusion ("densification") of the nylon 11 coatings was observed to occur from post-deposition heating, which continued after the initial particle impacts. These higher deposit temperatures degraded the coatings, as evidenced by a change in coating color from opaque gray to tan or dark brown.

Internal powder injection resulted in higher powder temperatures (and thus better splat morphology) than during external feed, even though the flame temperature was lower. The higher particle temperatures arose due to a longer dwell time and better jet trajectories, but the time was short enough that degradation

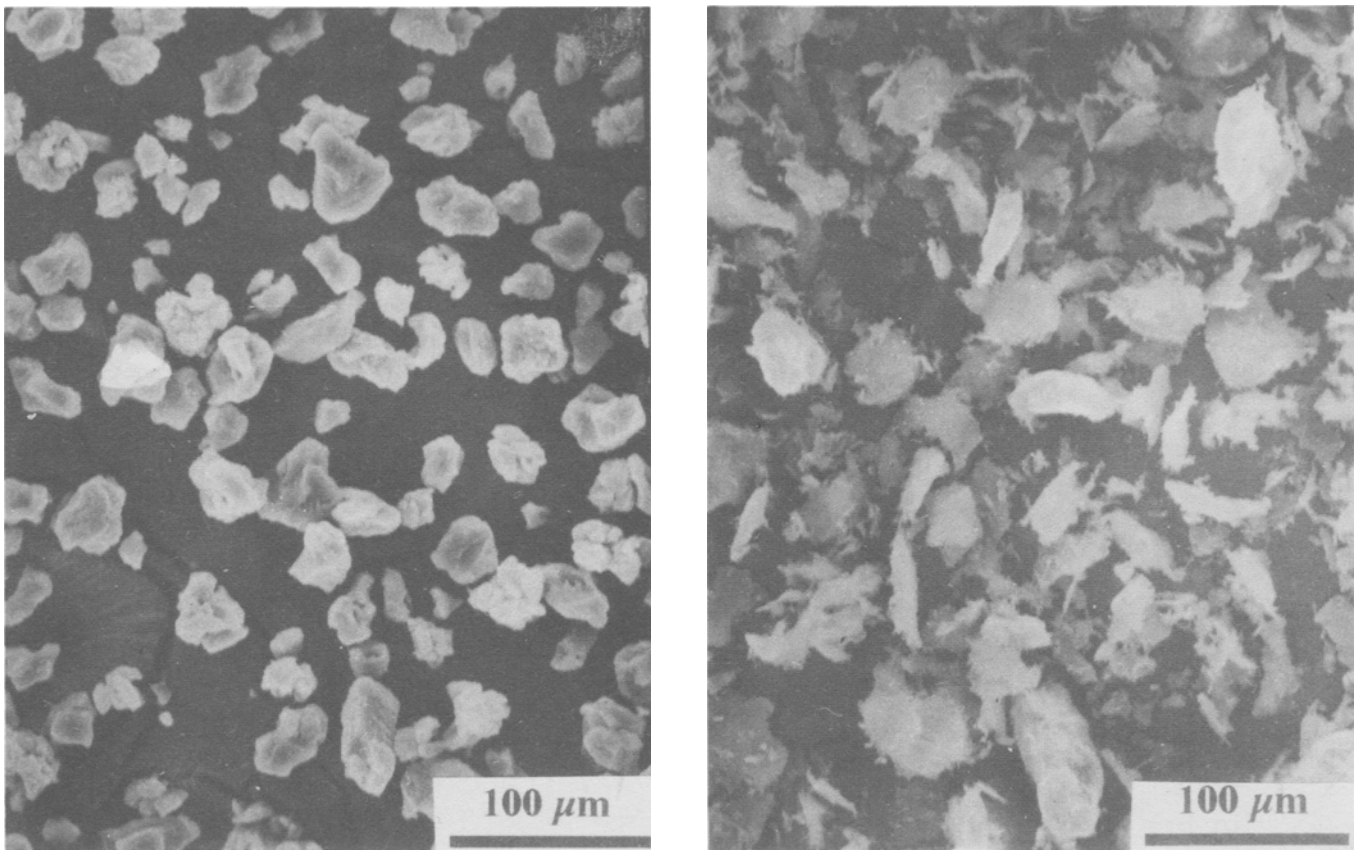

(a) (b)

Fig. 5 SEM micrographs of the nylon powder. (a) As received. (b) After ball milling with silica

did not occur, as evidenced by the small changes in measured coating viscosity (Table 3) and color. In addition to better splat behavior, the lower flame temperature kept the substrate from overheating and degrading the polymer after deposition.

The spray distance was found to be a critical parameter for two reasons. First, the spray distance determined the amount of heat input to the substrate. Second, the spray distance determined how long the particles were in flight and thus controlled their impact temperatures. The spray distance was varied from 150 to 250 mm (6 to 10 in.) for pure nylon. Figure 7 compares particles captured by the swipe test at 175 and 200 mm (7 and 8 in.). At 200 mm (8 in.), the particles deformed significantly upon impact, indicating good melting. At 175 mm (7 in.), particles were not deformed as much. A swipe test at 225 mm (9 in.) also indicated poor splat response.

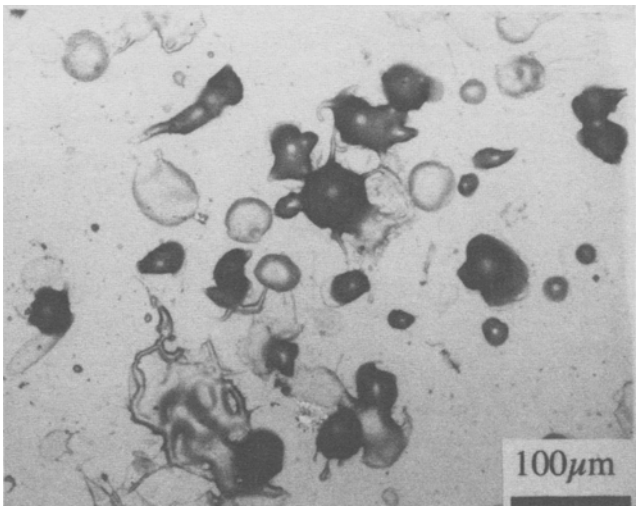

Fig. 6 Swipe test results for nylon powders sprayed using external feed, showing poor splatting

These results indicate there is a maximum distance after which the flame temperature, and thus the particles, begins to cool. At shorter distances, the particles did not have sufficient time to melt and the close proximity of the substrate to the flame caused degradation of the coatings after deposition. Therefore, an optimum spray distance of 200 mm (8 in.) was established using the pure nylon powders, which was maintained for deposition of all subsequent ceramic/polymer nanocomposite mixtures.

The fuel-to-oxygen ratio was changed to vary the overall particle impact temperature when necessary. It was found that optimum splat behavior occurred at nonstoichiometric ratios. Table 4 indicates the tested ratios that gave the best results for each mixture sprayed. Oxygen at levels lower than those reported in Table 4 caused degradation of the coating, whereas more oxygen resulted in insufficient splat deformation of larger particles. In the latter case, excess oxygen cooled the flame since it did not participate in combustion. As seen in Table 4, as the silica content increased, a closer-to-stoichiometric ratio (less excess oxygen to act as a cooling gas) was needed to achieve the higher temperature necessary to splat the particles. This is believed to be related to the higher apparent heat capacity of individual particles with silica particle additives, indicating that more thermal energy was required to heat these particles to their melt temperature. There was no difference in the fuel/oxygen ratio required for the hydrophilic and hydrophobic silica since the surface chemistry modifications did not change the bulk silica properties.

The 76 mm (3 in.) long nozzle was found to be optimal for particle heating and thus was used for most of the study. Results for the 153 mm (6 in.) long nozzle indicated that the increased dwell times caused overheating of the particles and resulted in darkened coatings, which indicated polymer degradation. Reduced spray distances to decrease particle dwell time outside the nozzle were tried, using the 153 mm (6 in.) nozzle, to compensate for the longer nozzle dwell time. However, the shorter spray distances caused substrate/coating overheating.

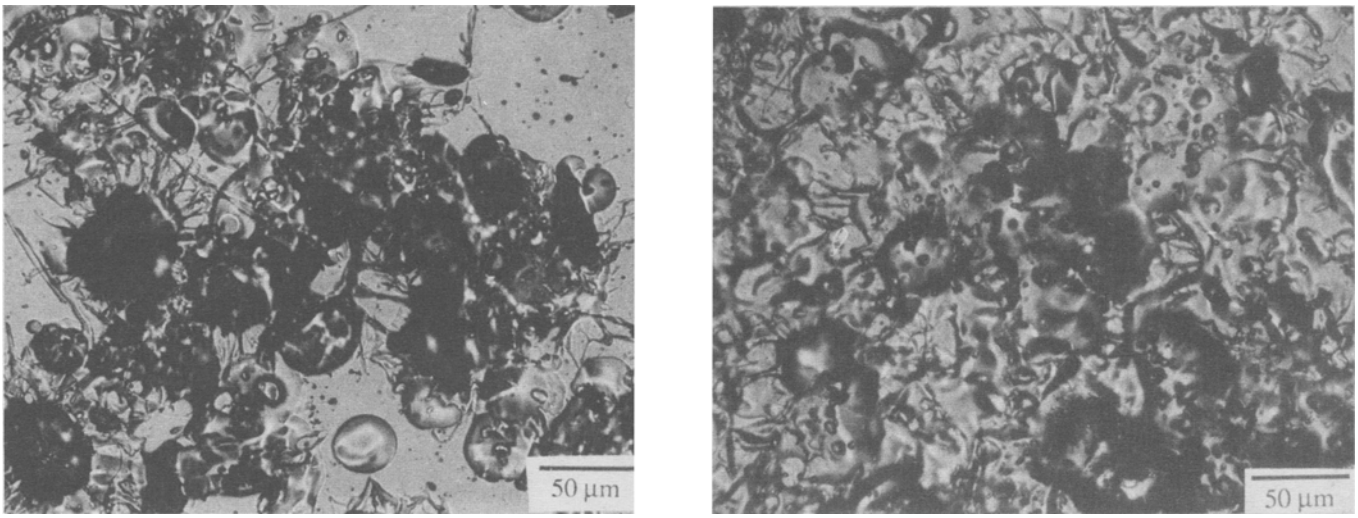

(a) (b)

Fig. 7 Swipe test results for composite powders sprayed at a distance of 175 mm (a) and 200 mm (b). The best splatting was observed at a spray distance of 200 mm

Substrate cooling was found to be an important coating process parameter since substrate temperature determined the post-deposition fusion, degradation, and adhesion mechanisms in the polymer coating. Coating analyses revealed that hot substrates caused excessive degradation while cool substrate temperatures, when combined with low flame temperatures, resulted in insufficient coating density. The solution was to use a water-cooled block to moderate substrate temperature, in conjunction with higher flame temperatures. In this way, coating postdeposition fusion and polymer degradation effects were limited while optimum in-flight particle melting was determined.

During these cooled tests, it was found that low substrate temperatures decreased coating adhesion, as evidenced by spalling. It was further observed that the bond between the coating and the substrate was improved on alumina-grit-blasted surfaces, because the roughness enhanced mechanical interlocking. Coating adhesion was qualitatively compared by mechanically removing the coating from the substrate. Adhesion was considered poor if the coating could be peeled off easily and in one piece. Good adhesion meant that the coatings had to be scraped off in small pieces.

The spray conditions that led to good polymer flow into substrate asperities resulted in the best adhesion (Fig. 8). Therefore, to enhance bonding, the substrate temperature was raised slightly before deposition by passing the flame over the substrate. It is important to note that the small substrates (25 by 76 mm) used in this study were not good heat sinks. Thus, chill blocks were required to better control coating temperatures. In industrial use, where larger structures would be sprayed, chill blocks would not be necessary because the increased mass would better maintain appropriate temperatures.

It is clear from the results that both in-flight melting and postdeposition fusion result in dense polymer coatings. However, there are two main reasons to control the density or quality of the coatings with parameters that promote in-flight melting instead of postdeposition fusion with hotter substrates. First, the in-flight heating process will make the coating process independent of substrate type. This is especially important in field applications, where large substrates cannot be easily heated. The second, more important consideration is the need to homogeneously distribute the nanoparticulate ceramic reinforcement particles through the polymer (nylon 11) matrix, which requires well-melted particles prior to impact.

Table 3 Change in inherent viscosity of nylon due to internal powder feed

Condition	Nylon, wt%	Hydrogen flow rate at 0.83 MPa, L/min	Oxygen flow rate at 0.83 MPa, L/min	Spray distance, mm	Inherent viscosity, cm^3/g
Not sprayed	100	N/A	N/A	N/A	0.83
Sprayed	100	400	600	200	0.9
Sprayed	100	400	600	225	0.9

Table 4 Spray parameters used to deposit nylon 11 and the composite coatings

Run No. (injection)(a)	Nylon, wt%	Silica, wt% (type)	Hydrogen flow rate at 0.83 MPa, L/min	Oxygen flow rate at 0.83 MPa, L/min	H_2/O_2 ratio(b)	Spray distance, mm
1 (internal)	100	0	450	600	0.75	200
2 (internal)	90	10 (hydrophobic)	500	600	0.83	200
3 (internal)	90	10 (hydrophilic)	500	600	0.83	200
4 (internal)	85	15 (hydrophobic)	550	600	0.92	200
5 (internal)	85	15 (hydrophilic)	550	600	0.92	200
6 (external)	90	10 (hydrophilic)	500	600	0.83	200

Constant parameters

Powder carrier gas	Nitrogen
Powder carrier gas flow	20 L/min at 0.69 MPa
Powder flow	9 rev/min
Substrate cooling	Water-cooled chill block
Number of cycles	3 cycles at 10 passes per cycle
Step size per pass	3.2 mm
Powder preparation	Composite ball milled for 48 h; vacuum dried at 80 °C for 24 h

(a) Runs 1 to 5 were sprayed while cooling the substrate using a water-cooled chill block. Run 6 was cooled using high-speed rotation of the substrate. (b) H_2/O_2 stoichiometric ratio is 2:1.

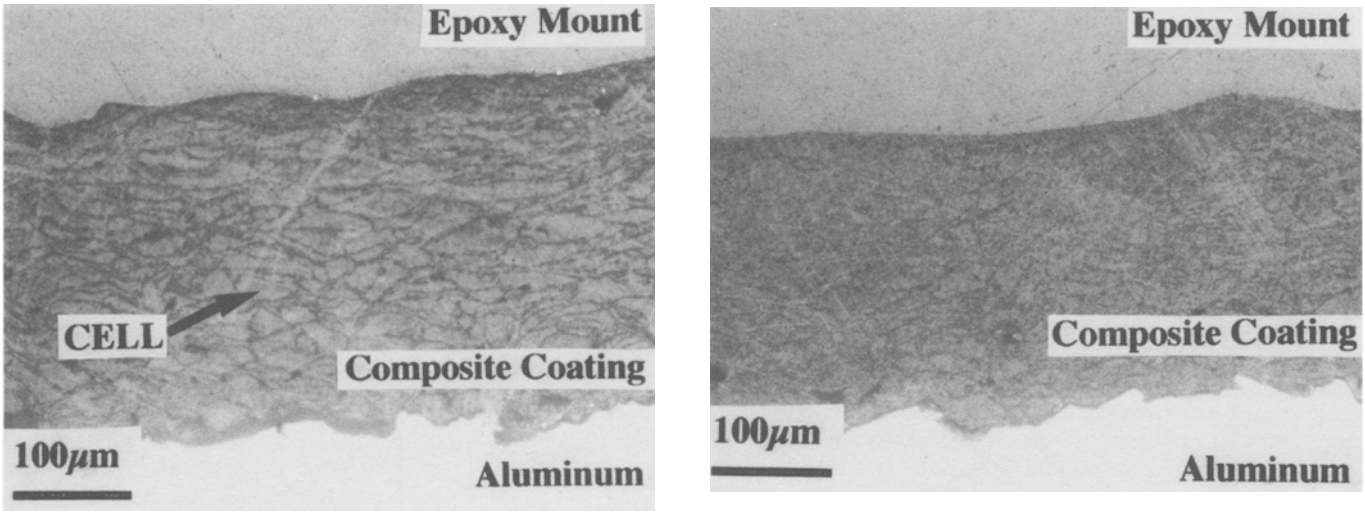

(a) (b)

Fig. 8 Composite coating microstructures that result from insufficient splatting (a) and good splatting (b). Note the cell structure that develops due to insufficient splatting.

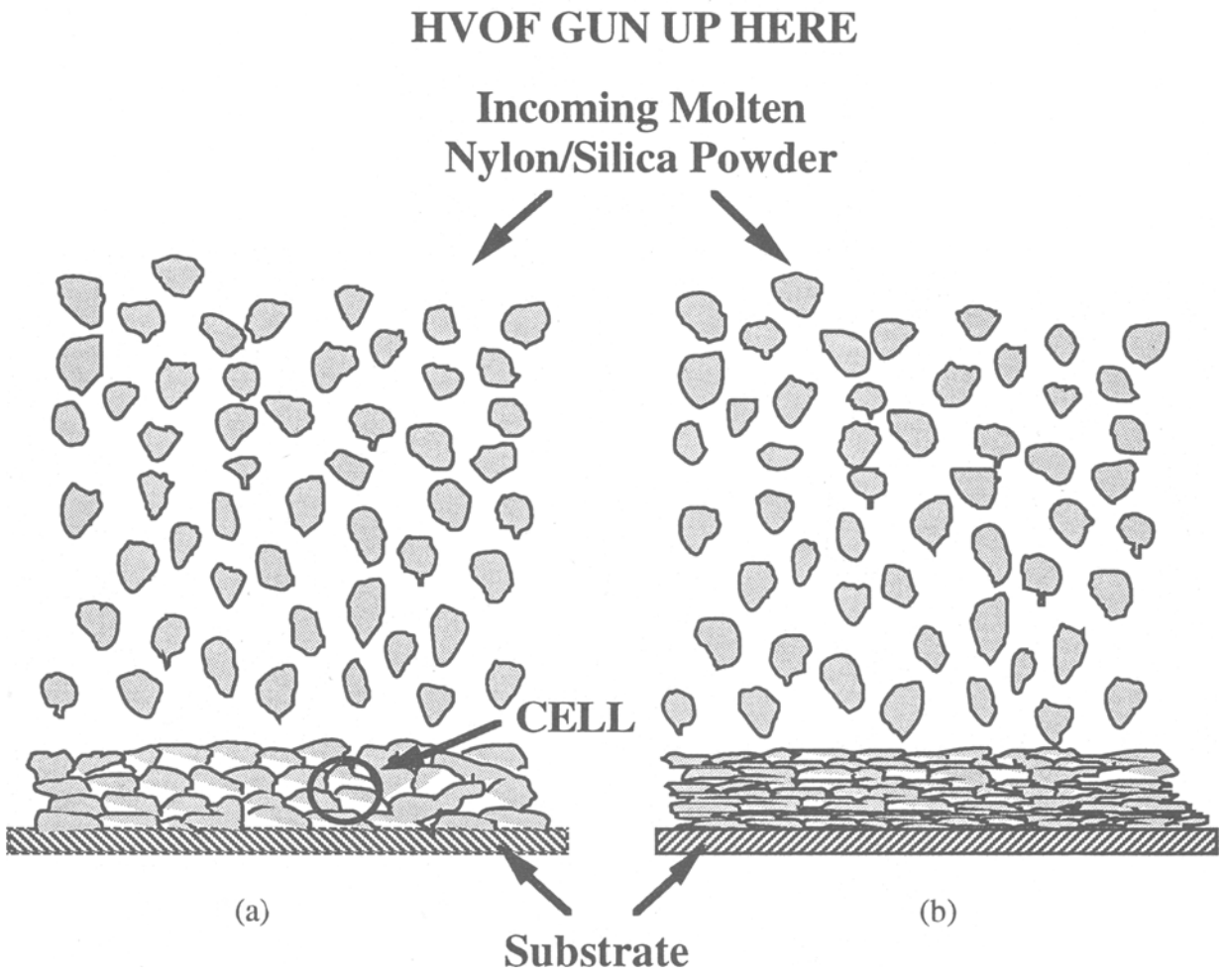

Fig. 9 Illustration of coating microstructure development. (a) Insufficient splatting, which results in poor distribution of the silica and a cell-type microstructure. (b) Good splatting, which results in better distribution and a loss of the cell-type microstructure

Figure 8 presents the coating microstructures that resulted from different particle heating process parameters. Figure 8(a) shows a coating produced by conditions that yielded insufficient melting. The silica has remained primarily at the outer surface of the still granular impacted nylon particles. The nylon powder particles, being poorly heat in flight, have remained largely undeformed, producing a coating with a cellular structure. Figure 8(b) depicts a spray condition with improved particle heating, leading to improved splat behavior and little or no cellular structure in the coating. In this case, it is believed that the powder particles splat against the substrate and deform sufficiently to bring the outer surface silica regions of the particles into close contact as the particles flatten. The cellular structures (Fig. 8a) were produced when the polymer particle did not significantly deform, leaving the silica-rich regions separated by an "unmolten" polymer core. Figure 9 schematically illustrates the coating microstructure development and silica distribution/coating densification for two cases: poor melting (Fig. 9a), which leads to cells, and good in-flight melting (Fig. 9b), which reduces or eliminates the cells and results in better silica distribution through the coating volume.

3.2 *Mechanical Behavior*

The POD sliding wear test and the scratch test were used to evaluate changes in coating mechanical properties related to the nanoparticle silica additions. These tests were sensitive to changes in particle loading and to the effects of silica particle surface chemistry. In the wear tests, the coating wear track cross-sectional area was measured using a profilometer and is shown for all the composite coatings in Fig. 10. After 15,000 revolutions, the pure nylon coating showed the highest wear, with a wear track area of approximately 68,000 μm^2. The nylon 11 coatings reinforced with 15 vol% hydrophobic silica exhibited the lowest wear, with wear track areas of approximately 30,000 μm^2. Wear resistance improved for 10 vol% hydrophobic and 10 vol% hydrophilic silica-reinforced coatings, with wear track areas of about 34,000 and 53,000 μm^2, respectively. Even greater wear resistance was found for the composites with 15 vol% loading, with wear track areas for the hydrophobic and hydrophilic silica/nylon composites of approximately 30,000 and 47,000 μm^2, respectively.

The wear track areas, plotted in Fig. 10, indicate that:

- Pure nylon coatings were the least wear resistant.
- Nanosize silica reinforcements improved the wear resistance in all cases.
- Increasing the volume percentage of nanoparticle silica reinforcement resulted in further improvement in wear resistance.
- Hydrophobic silica/nylon composite coatings were always more wear resistant that hydrophilic silica/nylon composite coatings.

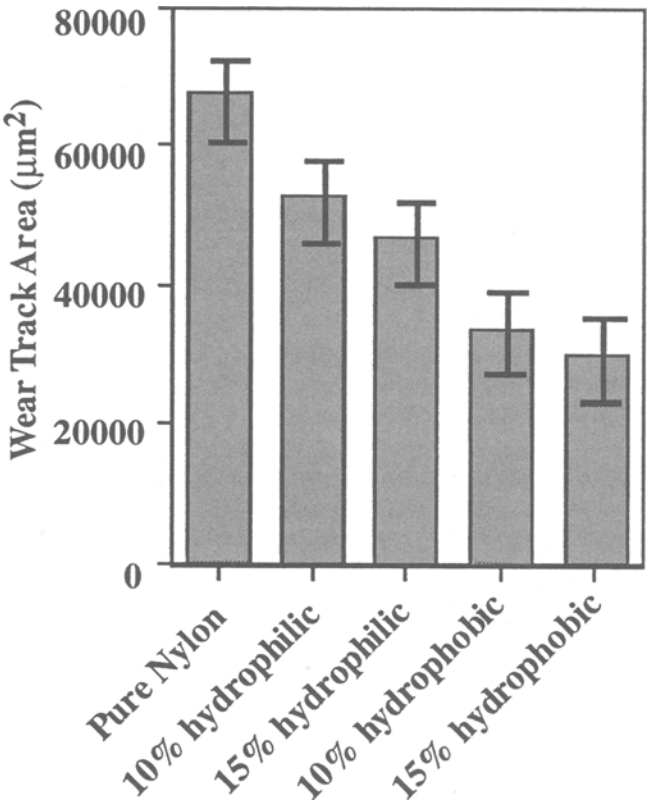

Fig. 10 Wear track area of nylon and nylon/silica composite coatings at several loading levels and as a function of silica surface chemistry

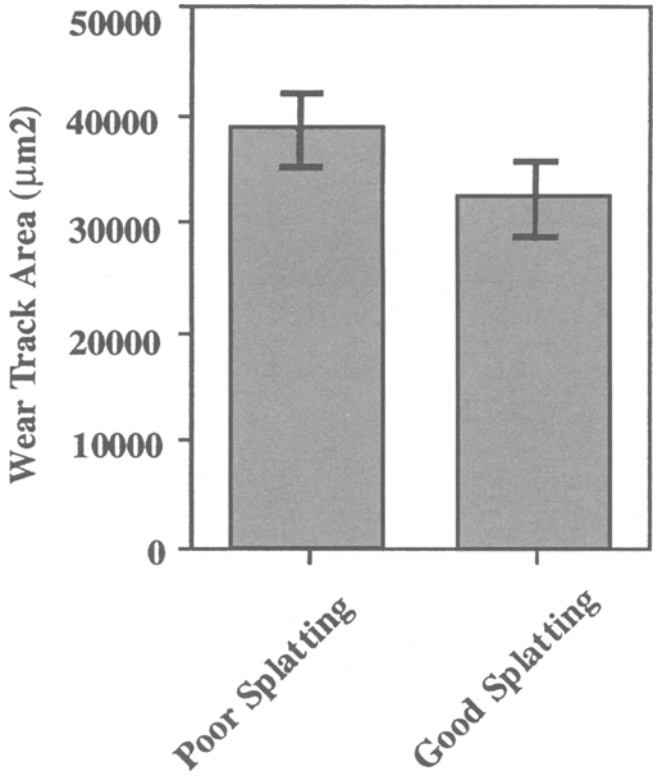

Fig. 11 Comparison of the wear track area for coating in Fig. 8(a), with poor silica distribution (poor splatting), and coating in Fig. 8(b), with good silica distribution (good splatting). Good distribution is important for obtaining maximum improvement in mechanical properties

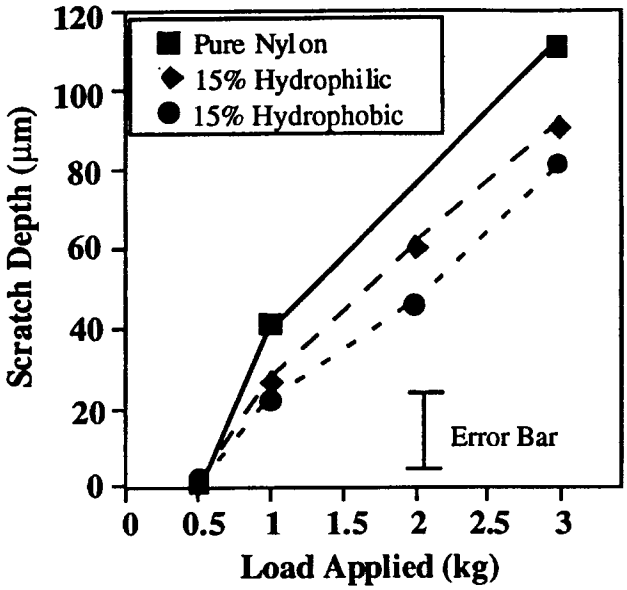

Fig. 12 Scratch test results for several composites showing the effect of silica loading and surface chemistry on scratch resistance

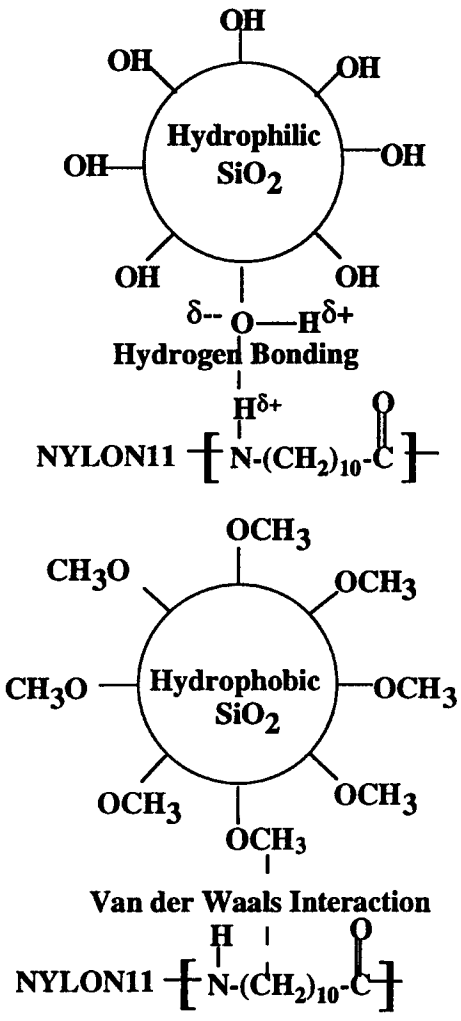

Fig. 13 Schematic of the hypothesized chemical interactions of the silica with the nylon that would affect mechanical properties

The wear test also demonstrated the effect of particle distribution on coating properties. Figure 8 shows two 10% hydrophobic silica-reinforced coatings: The coating in Fig. 8(b) exhibited good distribution compared to the poor distribution and the resultant cell structure of the coating in Fig. 8(a). Figure 11 compares the wear track areas for these two coatings. Note that after cycling for 15,000 revolutions, the coating with poor dispersion had approximately 15% greater wear than the other coating.

Figure 12 shows the scratch test results for several coatings and compares the effect of silica surface chemistry (hydrophilic or hydrophobic) and loading on scratch depth. Compared to pure nylon coatings, composites with 15% hydrophobic silica particles show a 30% reduction in scratch depth, while hydrophilic silica additions result in a reduction of approximately 15%.

The improvements in observed scratch and wear resistance from the addition of hydrophobic silica can be explained by exploring the possible interaction of hydrophobic and hydrophilic silica with nylon 11. Figure 13 shows that hydrophilic silica has a hydroxylated surface (OH groups), whereas hydrophobic silica has a predominantly methylated (CH_3 groups) surface. The hydroxyl groups (OH) have a tendency for polar interaction with the amide (NH_2) groups found in nylon 11. Correspondingly, the methyl groups of hydrophobic silica have a van der Waals interaction with the hydrocarbon linkages in the nylon 11. In the nylon 11 structure, CH_2 groups are more abundant (ten in every repeating unit) than the amide group (one in every repeating unit). Thus, it is likely that these hydrophobic interactions will be more pervasive, resulting in a stronger interaction between the particle and the matrix.

A second explanation is that the hydrophobic silica is dispersed better in the nylon 11. Hydrophobic surfaces would be less likely to agglomerate than hydrophilic surfaces and would thus make dispersion easier. It is not known which explanation is correct, but it is clear that surface chemistry is important in dictating coating performance.

It was observed that uneven silica distribution, which resulted in coating cell structures, reduced both scratch and wear resistance. It is well known that the larger the reinforcing particle size, the lower the yield stress and thus the scratch resistance (Ref 5). In the case of poor distribution, the reinforcing particles were more agglomerated and thus were acting as larger particles. In addition, there were large areas composed of pure nylon 11 which thus exhibited pure nylon 11 properties, reducing overall coating performance.

4. Summary

The results show that HVOF was a good method for depositing polymer and nanoparticulate ceramic-reinforced polymers. Several thermal effects must be balanced to achieve optimum nanoparticulate ceramic/polymer composite coatings using HVOF. For example, the particles must melt/soften sufficiently in flight to splat well against the substrate. Although a hot substrate led to post-deposition fusion, it did degrade the polymer—as evidenced by polymer viscosity and color changes. Correspondingly, the substrate must not be too cold, since the first polymer layers must flow to adhere to the substrate sufficiently to mechanically lock to substrate asperities.

For nylon/silica composite particles, good splat behavior was achieved using a JetKote HVOF gun (Stellite Coatings, Inc., Goshen, IN) with internal powder feeding, a 76 mm (3 in.) nozzle with a 8 mm ($^5/_{16}$ in.) diam outlet, an appropriate fuel/oxygen ratio (depending on ceramic content), and a spray distance of about 200 mm (8 in.). The substrate must be kept relatively cool during processing, but heated initially to provide an appropriate surface temperature to promote bonding of the first layer.

Pin-on-disk sliding wear and scratch tests showed marked improvements in wear resistance with the addition of nanosized silica filler. In both cases, hydrophobic silica improved the scratch and wear resistance more than the hydrophilic silica. The greatest improvement in properties was for the 15 vol% silica/nylon 11 composite which showed a 30% increase in scratch resistance and a 55% increase in wear resistance.

It was also observed that the HVOF spray conditions that affect in-flight particle heating can significantly affect coating properties. For example, a comparison of 10% hydrophobic silica-reinforced coating showed that after 15,000 cycles the wear track area of a well-dispersed (well-melted in flight) coating was approximately 15% less than coatings exhibiting cellular structures, when both coatings were tested under the same conditions.

Acknowledgments

The authors are grateful to the National Science Foundation for funding (grant No. DMI-9401052). They also thank Elf Atochem North America Inc. for donating the nylon 11 powder and viscosity measurements and Degussa Corporation for donating the silica powders.

References

1. M. Sumita, Y. Tsukumo, K. Miyasaka, and K.J. Ishikawa, Tensile Yield Stress of Polypropylene Composites Filled with Ultrafine Particles, *J. Mater. Sci.*, Vol 18, 1983, p 1758-1764
2. E.P. Giannelis, A New Strategy for Synthesizing Polymer-Ceramic Nanocomposites, *JOM*, Vol 44 (No. 3), 1992, p 28-30
3. T. Lan, P.D. Kaviratna, and T.J. Pinnavaia, On the Nature of Polyimide Clay Hybrid Composites, *Chem. Mater.*, Vol 6 (No. 5), 1994, p 573-575
4. P.H.T. Vollenberg and D. Heikens, Particle Size Dependence of the Young's Modulus of Filled Polymers, Part 1: Preliminary Experiments, *Polymer*, Vol 30, 1989, p 1656-1662
5. M. Sumita, Y. Tsukumo, K. Miyasaka, and K.J. Ishikawa, Effect of Reducible Properties of Temperature, Rate of Strain, and Filler Content on the Tensile Yield Stress of Nylon 6 Composites Filled with Ultrafine Particles, *J. Macromol. Sci. Phys.*, Vol B-22 (No. 4), 1983, p 601-618
6. Y. Bao, D.T. Gawne, D. Vesely, and M.J. Bevis, Formation and Microstructure of Plasma Sprayed Polyamide Coatings, *Surf. Eng.*, Vol 10 (No. 4), 1994, p 307-313
7. R.W. Smith and R. Knight, Thermal Spraying, Part I: Powder Consolidation—From Coating to Forming, *JOM*, Vol 47 (No. 8), 1995, p 32-39
8. R.J. Young and P.A. Lovell, *Introduction to Polymers*, Chapman and Hall, London, 1991, p 195-198